International Journal of Biological Macromolecules 321 (2025) 146607

Contents lists available at ScienceDirect

International Journal of Biological Macromolecules

journal homepage: www.elsevier.com/locate/ijbiomac

Modulating techno-functional and flavor binding characteristics of pea protein through ultrasound mediated dextran conjugation: Impact of power levels and underlying mechanism

Fatih Mehmet Yılmaz [a,b,*], Ahmet Görgüç [a,b], Sílvia de Lamo-Castellví [a,c], Sheryl Barringer [a,**]

[a] The Ohio State University, Department of Food Science and Technology, Columbus, OH 43210, USA
[b] Aydın Adnan Menderes University, Engineering Faculty, Department of Food Engineering, 09010 Efeler, Aydın, Türkiye
[c] Universitat Rovira i Virgili, Departament d'Enginyeria Química, Av. Països Catalans 26, Campus Sescelades, 43007 Tarragona, Spain

ARTICLE INFO

Keywords:
Protein modification
Volatiles in pea protein
Aroma binding of protein
Protein secondary structures
Sonication effect
Protein carbohydrate interaction
Ultrasound assisted conjugation

ABSTRACT

This study investigates the influence of ultrasound-assisted Maillard conjugation on the aroma-binding and techno-functional properties of pea protein–dextran conjugates. Despite increasing interest in enhancing plant protein functionality, the effects of conjugation on protein–aroma interactions, particularly under varying ultrasound intensities, remain largely unexplored. To address this gap, four ultrasound amplitudes (25–100 %) were compared with a traditional 15-min wet-heating method. Conjugation was confirmed through glycation degree, browning index, Maillard reaction indicators, and FT-IR spectral changes. Aroma profile and binding behavior were evaluated using headspace analysis via Selected Ion Flow Tube Mass Spectrometry (SIFT-MS). Ultrasound up to 50 % amplitude enhanced glycation efficiency and significantly improved solubility (from 35 % to over 71 %), oil-binding capacity, emulsification indices, and foaming properties, while reducing water-holding capacity. Although conjugation was a short-term process, the formation of Maillard-derived volatiles such as furans, alcohols, pyrazines, and sulfur compounds was observed, which declined at the highest ultrasound intensity. The interaction of octanal (aldehyde) and 2-octanone (ketone) with the protein was improved under optimal conjugation conditions in controlled aroma-binding assays. These changes were correlated with α-helix, β-sheet, and random coil content, as well as with denaturation temperature and enthalpy, zeta potential, solubility, and conjugation degree.

1. Introduction

Pea protein has gained considerable attention for its favorable nutritional profile, absence of cholesterol and lactose, and non-GMO status, making it popular among health-conscious consumers [1]. It is widely used in emulsion-based plant foods due to its foam stability, low allergenicity, high availability, and cost-effectiveness [2]. Moreover, it is rich in arginine and leucine—amino acids beneficial for muscle development—and shows relatively high bioavailability [3]. Today, pea protein ranks as the second most utilized plant-based protein globally, after soy [4]. However, low solubility and a beany flavor limit its broader application [5].

The production process, involving heat and pH adjustments, can alter protein conformation and reduce functionality [6]. Additionally, proteins are sensitive to environmental stresses such as pH shifts, heat, and shear forces, which further hinder their food applications [7]. Consequently, various modification strategies, including molecular-level techniques, have been proposed to improve plant protein functionality [8]. Among these, the Maillard reaction stands out for enhancing protein properties naturally and safely [9]. Controlled Maillard conjugation has been reported to improve solubility, foaming, water- and fat-binding capacities, and emulsifying ability [10,11]. It can also influence aroma-binding behavior by altering protein structure [5].

Wet heating is preferred over dry heating due to shorter processing times, but high temperatures (90–100 °C) may cause aggregation and reduce efficiency. Ultrasound-assisted Maillard conjugation has emerged as a promising solution; however, it can also lead to denaturation depending on intensity and duration [12]. Prior studies have

* Correspondence to: F. M. Yılmaz, Aydın Adnan Menderes University, Engineering Faculty, Department of Food Engineering, 09010 Efeler, Aydın, Türkiye.
** Corresponding author.
E-mail addresses: Yilmaz.65@osu.edu, fatih.yilmaz@adu.edu.tr (F.M. Yılmaz), Barringer.11@osu.edu (S. Barringer).

https://doi.org/10.1016/j.ijbiomac.2025.146607
Received 21 April 2025; Received in revised form 24 July 2025; Accepted 4 August 2025
Available online 6 August 2025

mostly investigated single ultrasound intensities and lacked focus on intensity-dependent effects in pea protein, especially regarding volatile compound formation.

Previous studies have investigated the effect of wet heating methods (ranging from 15 min to several hours) and examined the role of ultrasound in modifying various proteins [2,12–14]. However, most studies have focused on the time-dependent effects of ultrasound at a single intensity, with limited research exploring the impact of different ultrasound intensities—particularly in the modification of pea protein. Additionally, little is known about the volatile compounds formed during the Maillard reaction and how structural modifications influence the flavor-binding properties of proteins. Understanding these interactions is essential for designing plant-based protein ingredients with improved sensory and functional performance in food applications.

This study investigates the impact of ultrasound-assisted Maillard conjugation under the shortest feasible wet heating conditions, using four ultrasound amplitudes (25–100 %). Volatile compounds are analyzed via selected ion flow tube mass spectrometry (SIFT-MS), a highly sensitive and preparation-free method suitable for complex food matrices [15,16]. The goal was to evaluate how different ultrasound intensities affect protein functionality and volatile profiles, and to identify the optimal conditions for improving pea protein.

2. Materials and methods

2.1. Materials and chemicals

Pea protein (81.2 % protein content) was purchased from Naturiga Inc. (İstanbul, Türkiye), while dextran from *Leuconostoc* spp. (40 kDa), propylene glycol, o-phthaldialdehyde reagent solution, octanal (99 %), 2-octanone (98 %), and ethanol were obtained from Sigma-Aldrich (Merck KGaA, Darmstadt, Germany). Coomassie Brilliant Blue G-250, sodium phosphate dibasic, sodium phosphate monobasic and o-phosphoric acid were supplied by Thermo Fisher Scientific (Waltham, MA, USA), and bovine serum albumin was sourced from RPI (Mount Prospect, IL, USA).

2.2. Preparation of pea protein–dextran conjugates

2.2.1. Controlled heating Maillard conjugation

Pea protein powder and dextran (2:1, *w*/w) were mixed with 0.2 M sodium phosphate buffer (pH 7.0) at a total solid-to-solution ratio of 3 % (*w/v*) and stirred for 3 h. The mixture was further stirred overnight at 4 °C, then transferred to a 90 °C water bath for 15 min and cooled to an ambient temperature in an ice bath [17]. The resulting mixture was centrifuged at 4200 rpm at 4 °C for 15 min (Thermo Scientific Sorvall Legend XFR, USA), and the supernatant was subsequently freeze-dried (Labconco Kansas City, MO, USA) at −48 °C and 1.00 mbar for 48 h. The obtained powders were stored in glass jars at 0–2 °C.

2.2.2. Ultrasound-assisted Maillard conjugation

The same procedure as described above (2.2.1) was followed, with the exception that ultrasound treatment was applied as a pre-step in the Maillard conjugation process. The total heating time remained 15 min, including the duration of the ultrasound pre-treatment. The 200 mL of dispersions were placed in a 400 mL Borosilicate cylindrical glass container (77.5 mm inner diameter, 80 mm outer diameter, and 11.9 cm height) and treated for 5 min at 20 kHz using a Branson Sonifier 450 sonicator (Branson Ultrasonics, Danbury, CT, USA). The 1/2″ standard probe (Model 101–147-037R) was immersed two-thirds of its length from the top of the dispersion. The container was sealed with triple-layer Parafilm to prevent evaporation during ultrasonication. Ultrasound amplitudes of 25 %, 50 %, 75 %, and 100 % were applied separately, based on preliminary trials that identified 25 % as the minimum effective threshold and 100 % as a reference for high-intensity treatment. During ultrasound treatment, the temperature of the dispersions increased depending on the amplitude (e.g., ~39 °C at 25 %, ~66 °C at 100 %), after which they were immediately transferred to a water bath and heated to 90 °C. In all samples, the temperature was maintained at 90 °C for 15 min once this point was reached. The temperature changes during the operation were recorded to determine the acoustic intensity (I_a, W cm^{-2}) using Eq. (1) [18]:

$$I_a = \frac{m.C_p.\frac{dT}{dt}}{A} \quad (1)$$

where m is the sample weight (g), C_p is the heat capacity of the sample (3.95 J g^{-1} K^{-1}), dT/dt is the experimentally determined rate of temperature increase, and A is the surface area of the ultrasound-emitting surface (cm^2).

2.3. Analyses

2.3.1. Degree of glycation (conjugation)

The degree of conjugation (glycation) was measured using the OPA method [12]. A 50 μL aliquot of a 0.2 mg/mL sample dissolved in dH₂O was mixed with 1 mL of OPA reagent and incubated at 35 °C for 10 min. Following incubation, the absorbance was recorded at 340 nm, and the degree of glycation (*DG*) was calculated using the following equation (Eq. (2)):

$$DG = \frac{A_0 - A_t}{A_0}\, x\, 100 \quad (2)$$

where A_0 represents absorbance of protein alone; A_t represents absorbance of conjugates.

2.3.2. Assessment of Maillard reaction process

The conjugates were diluted with dH₂O ensuring consistency across all samples for comparison. The absorbance of each conjugate was measured at 304 nm and 420 nm using a UV–Vis spectrophotometer (Agilent Cary 60, Japan) and a quartz cuvette, with pure water as the blank reference [19].

2.3.3. Color difference and browning index

The L*, a*, and b* values of the conjugated samples were measured using a Chroma Meter (CR-400, Konica Minolta, Japan). The total color difference (ΔE) was calculated by comparing the color values of untreated samples (i.e., L_0*, a_0* and b_0*) using Eq. (3), while the browning index (*BI*) was calculated using Eqs. (4) and (5) [8].

$$\Delta E = \sqrt{[(L^* - {L_0}^*)^2 + (a^* - {a_0}^*)^2 + (b^* - {b_0}^*)^2]} \quad (3)$$

$$BI = [100 \times (X - 0.31)/0.17] \quad (4)$$

$$X = [(a^* + 1.75 \times L^*)/(5.645 \times L^* + a^* - 3.012 \times b^*)] \quad (5)$$

2.3.4. Relative protein solubility

Samples were dispersed at a concentration of 1 mg/mL (pH 7.0), stirred for 60 min at room temperature, and then centrifuged at 6000 rpm for 10 min. The supernatant (0.1 mL) was reacted with 1 mL of Coomassie Brilliant Blue dye for 15 min in the dark. Absorbance was measured at 595 nm. Protein concentration was determined using a BSA standard curve (0.05–0.5 mg/mL), and solubility was calculated using Eq. (6) [20].

$$\text{Protein solubility } (\%) = \frac{\text{protein concentration in supernatant}}{\text{protein concentration of initial solution}}\, x\, 100 \quad (6)$$

2.3.5. Water holding and oil binding capacity

A 0.1 g sample was mixed with 10 mL distilled water (for water holding capacity) or a 0.05 g sample with 2 mL sunflower oil (for oil

binding capacity). The mixtures were vortexed for 10 s every 5 min for a total of 30 min, then centrifuged at 5000 *g* for 10 min. Water holding capacity (*WHC*) and oil binding capacity (*OBC*) were calculated using Eq. (7) [21].

$$\text{WHC or OBC (g/g)} = \frac{\text{Weight of sediment (g)}}{\text{Weight of dry sample (g)}} \quad (7)$$

2.3.6. Emulsion activity and stability

Emulsion properties were determined according to Erdogdu et al. [21]. A 0.05 g sample and 5 mL dH_2O (1 %; *w/v*) were homogenized at 10,000 rpm for 30 s, then 5 mL sunflower oil was added and mixed for 2 min. The emulsion was centrifuged at 3000 *g* for 5 min, and the final emulsion layer was recorded. The emulsion was heated at 80 °C for 30 min, then centrifuged again. Emulsion activity (*EA*) and stability (*ES*) were calculated using Eqs. (8) and (9), respectively.

$$\text{Emulsion activity (\%)} = \frac{\text{Emulsion volume (mL)}}{\text{Total volume (mL)}} \times 100 \quad (8)$$

$$\text{Emulsion stability (\%)} = \frac{\text{Emulsion volume after heating (mL)}}{\text{Total volume (mL)}} \times 100 \quad (9)$$

2.3.7. Foam capacity and stability

Foam properties were determined according to Rawat and Saini [22]. A 0.05 g sample was mixed with 5 mL dH_2O and homogenized at 10,000 rpm for 2 min. The total volume was recorded before and after homogenization (V_1 and V_2), and foam capacity (*FC*) was calculated using Eq. (10). The mixture was left at room temperature for 30 min, and foam stability (*FS*) was calculated using Eq. (11), based on the final volume (V_3).

$$\text{FC (\%)} = \frac{V_2 - V_1}{V_1} \times 100 \quad (10)$$

$$\text{FS (\%)} = \frac{V_3 - V_1}{V_1} \times 100 \quad (11)$$

2.3.8. ζ-potential

Samples were prepared at 1 % concentration in dH_2O and mixed by vortex for 60 s. ζ-potential was measured at 25 °C using a zetasizer (Anton Paar Litesizer 500, Austria).

2.3.9. FT-IR spectra and secondary structure content

Powders were analyzed with an FT-IR spectrophotometer (Agilent 4500a, Malaysia). Spectra (1600–1700 cm^{-1}) were normalized, smoothed, 2nd-derivatized, and Gaussian-fitted using OriginPro 2025 to estimate structural components [23].

2.3.10. Differential scanning calorimetry (DSC)

Using a PerkinElmer DSC 6000, ~5 mg powder was heated from −40 to 120 °C at 10 °C/min under nitrogen (20 mL/min). T_g, T_d, and ΔH were calculated via Pyris software.

2.3.11. SIFT-MS volatile analysis

Powders were first dissolved in water:propylene glycol (80:20, v:v) to 0.5 % (w:w). To determine the natural volatile content, the protein solutions were initially analyzed. For flavor binding analysis, octanal and 2-octanone were added separately to the same protein solutions at 1 % (*w*/w) relative to protein, using individual 10 g/L ethanol stock solutions. All samples were adjusted to pH 7.0, vortexed, sealed in Pyrex bottles, and analyzed using a SIFT-MS (SYFT Voice200ultra). Headspace volatiles were compared with blank bottles [24]. Triplicates were analyzed. Flavor binding capacity was calculated using Eq. (12):

$$\textit{Flavor binding capacity} = \frac{V_1 - V_2}{V_1} \quad (12)$$

where V_1 is the headspace concentration of 2-octanone in the absence of protein; V_2 is in the protein solution.

2.4. Statistical analysis

All treatment groups were independently prepared in duplicate (i.e., two independent sample preparations), and each sample was analyzed in triplicate. Reproducibility between the duplicate preparations within each group was assessed using an independent samples *t*-test, and no significant differences were observed ($P > 0.05$). Results were expressed as mean ± standard deviation. Data were analyzed via ANOVA using SPSS 15.0. Tukey's test ($P < 0.05$). Relationships among variables were evaluated using Pearson correlation and visualized as a heatmap in Python.

3. Results and discussion

3.1. Ultrasound intensity and evidence of conjugation

The corresponding average ultrasound intensities for 25, 50, 75, and 100 % amplitudes were 15.9, 22.4, 32.6, and 43.3 W cm^{-2}, respectively (Table 1). Evidence of conjugation was assessed through the degree of conjugation, UV–visible absorbance measurements at 304 and 420 nm, browning index, and FT-IR spectral analysis.

3.2. Conjugation degree, absorbance-based Maillard reaction product estimation, and browning index

When the degree of glycation was first evaluated (Fig. 1A), it was found to be 19.8 % with conventional wet heating. This value increased significantly to 43.7–48.2 % when ultrasound amplitudes of 25 % and 50 %, corresponding to an intensity of 15.9–22.4 W cm^{-2}, was applied. This notable enhancement is attributed to the instantaneous and localized generation of extremely high temperatures and pressures, which are subsequently damped [12]. Such conditions promote structural changes in the protein, including unfolding and bond displacement, thereby increasing its reactivity in the Maillard reaction [2]. However, when ultrasound intensities exceeded this range, the degree of glycation decreased, resulting in values similar to the control ($P > 0.05$). Specifically, ultrasound amplitudes of 75 % and 100 %, corresponding to intensities of 32.6 and 43.3 W/cm^2, resulted in glycation degrees of 25.4 % and 16.9 %, respectively. This decline suggests that excessively high ultrasound intensities can damage the protein structure, weaken bonds, and reduce the tendency for conjugation [25].

The measurement of protein solutions at 304 nm and 420 nm provides insight into the progression of the Maillard reaction, with absorbance at 304 nm generally corresponds to intermediate compounds and 420 nm with melanoidin formation [19]. It should be noted that the absorbance at 304 nm is only an indirect indicator of Maillard reaction progress, commonly associated with carbonyl-containing intermediate products. In the native (untreated) protein, minimal levels of absorbance values indicate limited initiation of the Maillard reaction (Fig. 1B). Low-intensity ultrasound (25 %) enhances the accumulation of non-specific

Table 1
Experimentally determined acoustic intensities (I_a) at different ultrasound amplitude levels.

Amplitude (%)	Acoustic intensity (W cm^{-2})
25	15.9 ± 0.7
50	22.4 ± 1.9
75	32.6 ± 2.2
100	43.3 ± 3.1

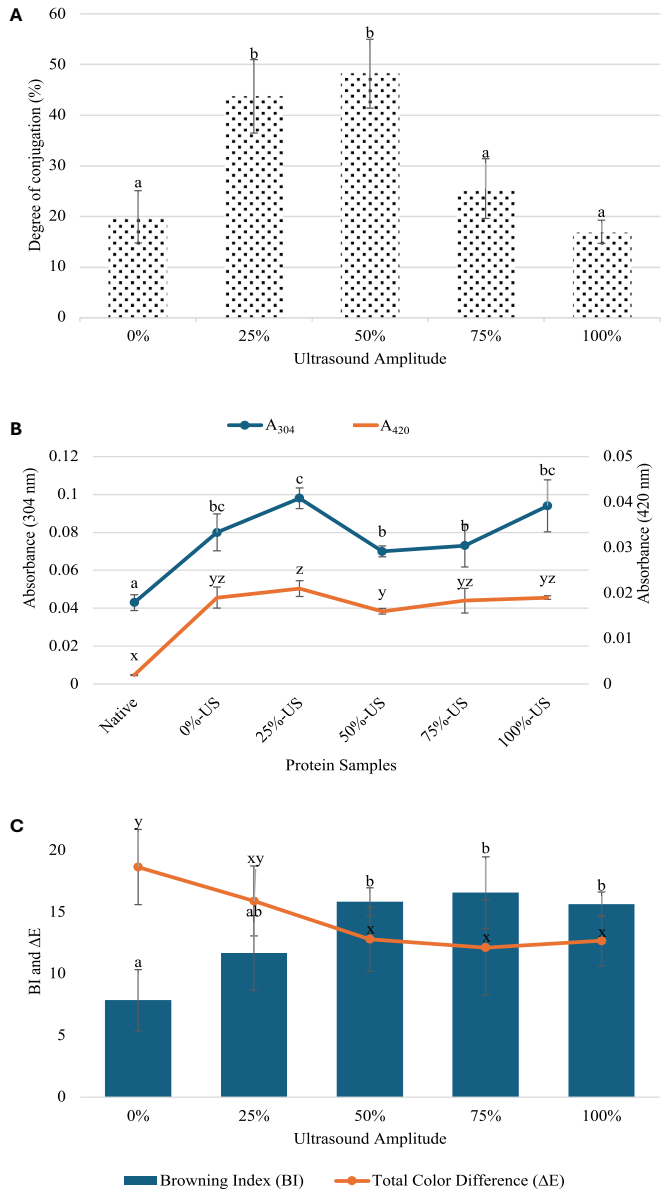

Fig. 1. Effect of wet heating (0 %) and ultrasound (US)-assisted conjugation (25–100 % amplitudes) on the degree of conjugation (A), UV absorbance of protein samples at 304 nm and 420 nm (B), and browning index (BI) and total color difference (ΔE) (C). Different letters (a–c or x–z) indicate statistically significant differences among the samples ($P < 0.05$).

Maillard intermediates, suggesting an acceleration of Maillard reaction. Conversely, higher ultrasound levels (50 % and above) reduce A_{304} values, possibly indicating their conversion to advanced Maillard products. Although absorbance associated with advanced Maillard products (A_{420}) at higher ultrasound intensities, the rise is not significant, suggesting a potential limitation of the Maillard reaction beyond a certain point [26,27].

Although A_{304} is a key contributor to Maillard conjugation, our results indicate it is not the sole factor determining conjugation degree. While conjugation increased at 25 % and 50 % ultrasound power levels, it declined at higher powers. In contrast, A_{304} showed a non-parallel trend, increasing at 25 %, decreasing at 50 %, and rising again at 100 % US. A similar pattern has also been observed in other studies. Fu et al. [12] reported no direct correlation between the degree of conjugation and changes in absorbance values, attributing this to the physical and mechanical effects of ultrasound. Likewise, Jiang et al. [28] found similar trends that these absorbance values did not consistently correspond with conjugation degree.

The browning index (BI) is a key indicator of Maillard conjugation, reflecting the progression of the reaction relative to the starting protein [22]. With conventional wet heating, the BI was 7.9 (Fig. 1C). Ultrasound treatments at 25 % - 100 % ultrasound amplitudes resulted in BI values of 11.7, 15.9, 16.6, and 15.6, a statistically significant increase ($P < 0.05$). The 25 % ultrasound application shows a relative increase compared to the classical method but remains lower than the 50 % and 75 % ultrasound treatments, despite being statistically in the same group. Fu, Yu, et al. [2] also reported a higher BI compared to traditional wet-heating treatment, which may be attributed to the high-intensity shear field induced by ultrasound, promoting the formation of intermediate and final protein reaction products.

The total color difference is highest in the conventional heating method (18.6) (Fig. 1C). However, this difference is significantly reduced with ultrasound. In ultrasound treatments, the initially light-toned samples darkened slightly, which reduced the overall color difference from the native protein. This resulted in a significant discrepancy between the total color difference and the browning index. Ultrasound generates cavitation in liquid media through intense sound waves [21]. This cavitation phenomenon can accelerate the Maillard reaction by enhancing protein-carbohydrate conjugation [8].

3.3. FT-IR analysis

In the FT-IR spectrum (Fig. 2A), the Amide *I* (1600–1700 cm^{-1}) and Amide II (1500–1600 cm^{-1}) regions of the untreated protein sample exhibit the highest absorbance with prominent peaks. The Amide *I* band is attributed to the C═O (carbonyl) stretching vibration, while Amide II corresponds to the N—H bending and C—N stretching vibrations [29]. A decrease in absorbance in these regions in ultrasound-generated conjugates suggests changes in the secondary structure of the protein. The sharp decrease in intensity at the Amide bands is likely due to the formation of a Schiff base, an intermediate Maillard reaction product formed between the amino groups of the protein and the reducing end of dextran [30].

A significant increase in absorbance or the appearance of new peaks in the 1000–1150 cm^{-1} region indicates formation of Maillard conjugates in the presence of dextran [28]. This region corresponds to the glycosidic bonds (C-O-C). In the untreated sample, the 1000–1150 cm^{-1} region shows very low absorbance, while the sample with the highest absorbance around 1100 cm^{-1} likely contains the most dextran and exhibits successful conjugation. This result correlates well with the degree of glycation and A_{304}. The 930–940 cm^{-1} region is associated with the characteristic O—H bending vibration, which may indicate the presence of carboxylic acids [31], likely formed after Maillard conjugation [32]. The 850 cm^{-1} region, which shows tyrosine interactions, also exhibits a distinct peak increase under ultrasound treatment. These interactions are typically linked to structural changes or cross-linking mechanisms of proteins [33]. Moderate levels of ultrasound (e.g., 25–50 %) likely open the protein surface and increase interaction with dextran. However, ultrasound at very high amplitudes (e.g., 100 %) may lead to protein denaturation or aggregation, reducing conjugation efficiency as protein solubility and the accessibility of reactive groups diminish [34]. It should be acknowledged that the current study does not provide direct evidence (e.g., particle size distribution or microscopic observations) for protein aggregation; rather, the interpretation is based on theoretical considerations and existing literature.

The Amide I region data of the protein spectrum was analyzed to estimate the percent secondary structures of protein samples (Fig. 2B). The highest percentage of secondary structure in the protein samples was attributed to β-sheet structures (Fig. 2C). This is coherent with the results of Jiang et al. [27] Upon dextran conjugation, the β-sheet content decreased, with the lowest values observed in samples treated with classical heating and 25–50 % ultrasound amplitudes. Beyond 50 %

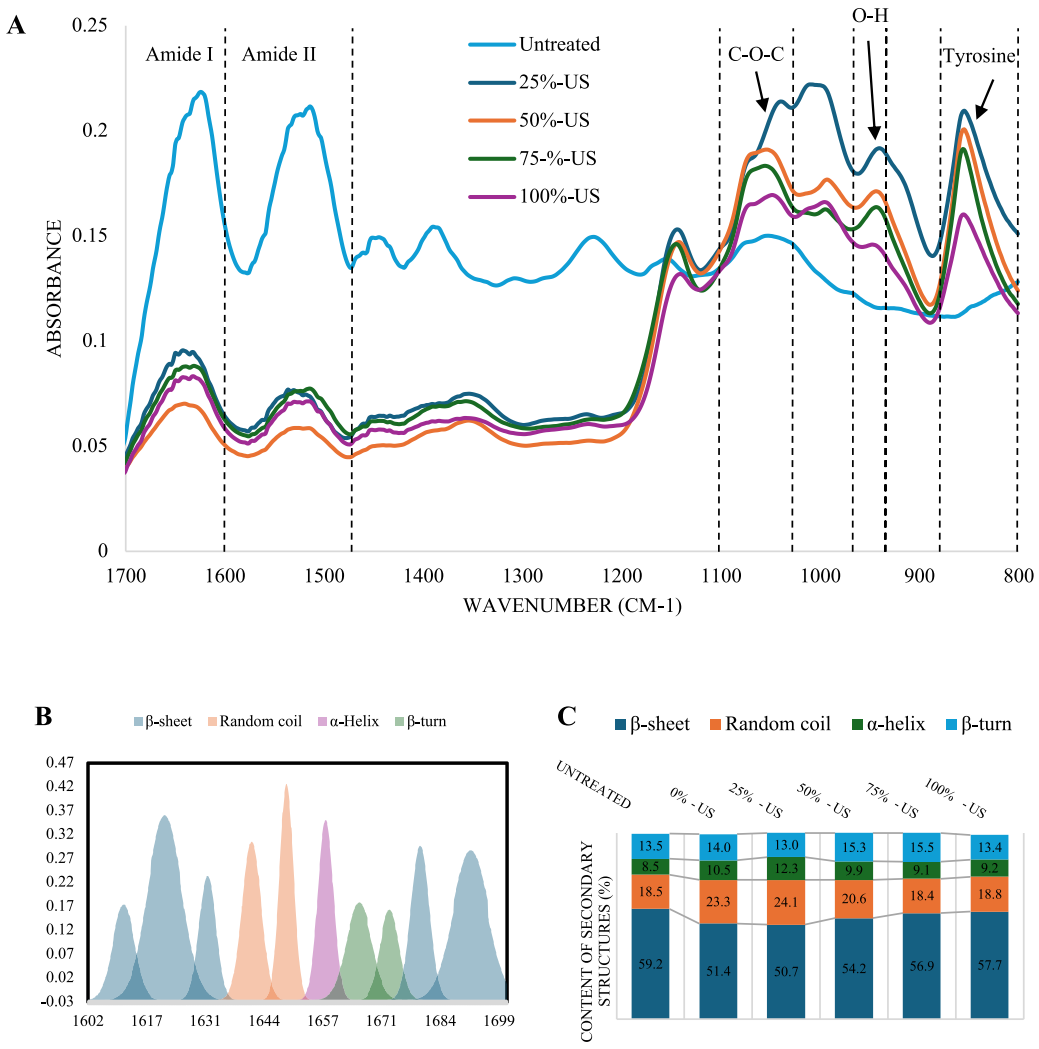

Fig. 2. Fourier transform infrared (FT-IR) spectroscopy of untreated and dextran conjugated protein samples (A), sample curve-fitted inverted second-derivative of the amide I region (B), and content or percentages of secondary structures of protein samples (C).

ultrasound, this decrease was less pronounced. In contrast, the α-helix content increased following Maillard treatment, particularly in samples treated with classical heating and 25 % ultrasound, suggesting that hydrogen bonds were disrupted by the reaction. Similar structural changes have been reported in whey protein-dextran conjugates, where increased α-helix content was linked to improved protein stability [30]. The reduction in β-sheet content indicates the breakdown of intermolecular and intramolecular interactions, resulting in a looser protein structure with greater steric hindrance. The binding of bulky, branched polysaccharides such as dextran can disrupt regular β-sheet structures by occupying space between protein chains, leading to more irregular and amorphous structures [35] Random coil structures, known for their flexibility, were most abundant in the 25 % ultrasound-treated sample. This flexibility enhances protein-polysaccharide interactions and appears to be significantly influenced by the conjugation process. As ultrasound intensity increased, α-helix and random coil content gradually decreased, while β-sheet content steadily increased. This trend can be attributed to the intensified cavitation effect at higher ultrasound intensities, which induces denaturation, aggregation, and excessive unfolding of the protein structure. Under such conditions, some protein chains may be forced to associate, promoting aggregation and partial refolding [36]. The FT-IR results, including both spectral analysis and secondary structure content, provided compelling evidence for the successful conjugation of protein with dextran and also demonstrated a distinct effect of varied ultrasound intensities.

3.4. Thermal behavior and zeta potential

The peak transition temperature (T_p), enthalpy (ΔH), and glass transition temperature (T_g) values are presented in Table 2. The T_p value shows a slight decrease following Maillard conjugation, especially at 75 % ultrasound treatment. The enthalpy values indicate an exothermic reaction, which may suggest disruption of hydrophobic interactions and possible aggregation, while dextran conjugation may promote a folded

Table 2
Differential scanning calorimetry (DSC) analysis results (T_p: Peak or denaturation temperature; ΔH_d: Denaturation enthalpy; T_g: Glass transition temperature; US: Ultrasound)*

Sample	T_p	ΔH_d	T_g
Native	69.9 ± 2.5^{b}	-168.7 ± 9.5^{c}	19.9 ± 1.1^{c}
0 %-US	67.5 ± 3.0^{ab}	-103.6 ± 19.4^{ab}	17.2 ± 0.7^{bc}
25 %-US	62.4 ± 3.9^{ab}	-92.9 ± 0.1^{a}	15.1 ± 1.5^{b}
50 %-US	62.3 ± 2.2^{ab}	-95.1 ± 2.1^{a}	18.3 ± 1.7^{bc}
75 %-US	58.9 ± 2.3^{a}	-116.4 ± 9.2^{b}	10.7 ± 1.6^{a}
100 %-US	70.6 ± 6.5^{b}	-107.7 ± 3.4^{ab}	10.3 ± 1.2^{a}

* Data are presented as mean ± standard deviation. Different uppercase letters denote statistically significant differences between mean values within the same column.

or aggregated structure [37]. The glass transition temperature (T_g) is a key marker for the storage stability of powder products [38]. In this study, ultrasound treatment at amplitudes of 75 % and above resulted in a considerable reduction in T_g, which may indicate reduced structural stability and increased molecular mobility, potentially compromising the long-term stability of the protein.

The effect of ultrasound at different power levels during conjugation on the zeta potential is shown in Fig. 3A. The ζ-potential value reflects the surface charge of protein samples [23]. While Maillard conjugation is generally reported to significantly increase the zeta potential due to enhanced functional properties of proteins [28], the results in this study suggest a different trend. Given the natural distribution of amino acids in pea protein, the presence of more negative charges is expected, while dextran, with its positive charges, interacts with the protein, leading to a decrease in zeta potential. This decrease can be explained by the binding of dextran, a large and flexible molecule, to energy-dense regions on the protein surface, reducing bond energy in those regions. Consequently, conjugation may neutralize surface charges, promoting a transition from a compact structure to a more open yet stable conformation [39]. Notably, the samples treated with 25 % and 50 % ultrasound amplitudes showed the lowest zeta potential values, which aligns with the higher degree of conjugation observed in those samples. Similar to our findings, Xie et al. [40] reported that conjugation reduced the zeta potential compared to ultrasound treatment alone. Furthermore, in our study, the slight increase in zeta potential observed at higher ultrasound power levels may be attributed to the increased specific surface area and the presence of additional surface negative charges induced by ultrasound treatment.

3.5. Solubility and emulsifying properties

Solubility and emulsifying properties are two major weaknesses of pea proteins [39]. The low solubility of pea protein is attributed to its low content of water-soluble albumins and the predominance of globulins, which are less soluble. While soybean, the most widely used plant-based protein source, exhibits good solubility, pea protein, as an alternative, shows significantly lower solubility. The untreated pea protein in this study had a solubility of 34.7 % (Fig. 3B). In accordance with previous reports, both controlled Maillard conjugation and ultrasound treatment improved pea protein solubility. Conjugation with dextran alone (classical heating) increased the solubility to 44.7 %, whereas dextran conjugation combined with ultrasound enhanced solubility up to 71 %. This improvement can be attributed to structural changes in the protein caused by dextran conjugation, which increase protein-water interactions [39]. Additionally, the intense mechanical shear forces generated by ultrasonic cavitation may disrupt the globular structure and inhibit protein refolding, further reducing particle size by enhancing collisions between protein aggregates [39].

However, at ultrasound power levels of 50 % and above, solubility decreased. This decline may result from excessive sonication effects, causing protein reaggregation. Prolonged exposure to intense ultrasound power may accelerate the advanced stage of the Maillard reaction, where crosslinking between dicarbonyl compounds leads to reduced solubility [22]. These findings are consistent with the absorbance-based indicators of Maillard reaction progression (Fig. S1). Furthermore, protein denaturation may have contributed to the reduced solubility observed at higher ultrasound intensities. A similar trend was reported in previous studies [39,41], where ultrasound treatment reduced solubility beyond a certain power threshold, consistent with our results.

Compared to untreated pea protein, the emulsion activity of dextran conjugates prepared using wet heating or ultrasound treatment significantly increased ($P < 0.05$) (Table 3). However, conventional conjugation (wet heating) led to a decrease in emulsion stability (from 46.32 % to 40.15 %). In contrast, ultrasound treatment significantly improved emulsion stability (approximately 56 %). In most similar studies, emulsion activity and stability exhibit a strong positive correlation, meaning both tend to increase simultaneously [2,27,37,42]. However, in this study, while conventional conjugation enhanced emulsion activity, it reduced emulsion stability. Dextran conjugation improved the surface activity of proteins, enhancing their emulsifying capacity. However, as discussed in the following section, the substantial reduction in water holding capacity may have limited water retention, leading to lower emulsion stability. It has also been suggested that there is an interdependent relationship between the water and oil retained by proteins, particularly in emulsified systems, where changes in water-holding capacity may influence oil-binding capacity, and vice versa [22]. Despite this, ultrasound treatment significantly improved protein-fat-water interactions [43], resulting in a marked enhancement in emulsion stability. These findings clearly demonstrate the synergistic effect of dextran conjugation and ultrasound treatment.

3.6. Water holding, oil binding and foaming properties

Table 3 presents the results for water holding capacity (WHC), oil binding capacity (OBC), foaming capacity (FC), and foaming stability (FS). A decline in WHC was observed when conjugation treatments were applied to pea protein. During conjugation, some hydrophilic groups on the surface of pea protein may covalently bind to dextran, leading to structural modifications. This could reduce the number of free hydrophilic groups available for water binding, thereby lowering WHC. Additionally, the increase in hydrophobic regions on the protein surface after conjugation is another significant factor [37,44]. The increase in hydrophobic regions may have promoted protein-protein interactions rather than protein-water interactions, resulting in reduced WHC. However, ultrasound treatment significantly improved WHC compared to the conventional conjugation method, though it did not fully restore it to the level of the untreated protein. High-energy sound waves may have altered the protein structure, exposing more water-binding sites. Regarding OBC results, all protein-dextran conjugates exhibited higher

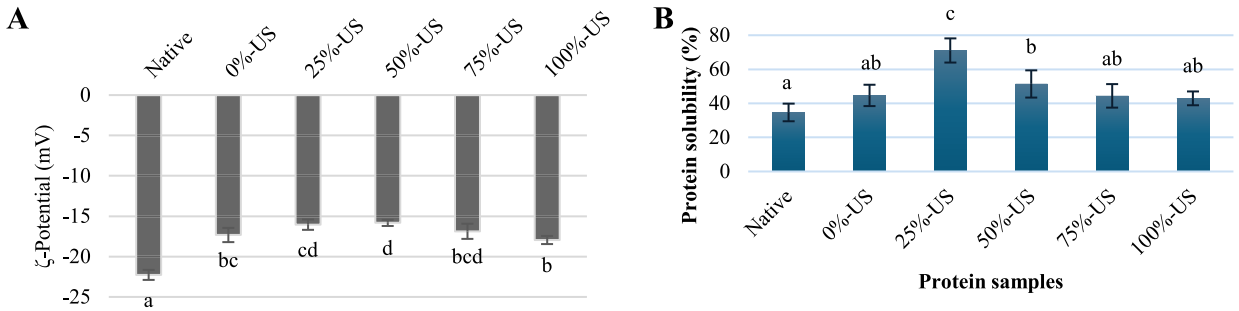

Fig. 3. Effectiveness of protein conjugation on the zeta (ζ) potential (A) and solubility (B) of pea protein. *Native* represents untreated pea protein, *0 %-US* indicates wet heating conjugation, and *25 to 100 %-US* corresponds to ultrasound conjugations at varied amplitudes. Different letters (a-d) indicate statistically significant differences ($P < 0.05$).

Table 3
Effect of conjugation method on the emulsion activity (EA), emulsion stability (ES), water holding capacity (WHC), oil binding capacity (OBC), foam capacity (FC) and foam stability (FS)*.

Sample	EA (%)	ES (%)	WHC (g/g)	OBC (g/g)	FC (%)	FS (%)
Native	51.6 ± 1.3^{a}	46.3 ± 0.4^{b}	4.11 ± 0.04^{d}	2.91 ± 0.17^{a}	52.5 ± 2.5^{a}	15 ± 4.1^{a}
0 %-US	61.3 ± 1.3^{c}	40.2 ± 1.3^{a}	0.87 ± 0.06^{a}	5.74 ± 0.57^{b}	95 ± 4.1^{b}	80 ± 0^{b}
25 %-US	56.9 ± 1.3^{b}	56.0 ± 1.3^{c}	2.13 ± 0.10^{b}	7.30 ± 0.32^{c}	95 ± 4.1^{b}	80 ± 0^{b}
50 %-US	59.1 ± 0.9^{bc}	56.9 ± 0.4^{c}	2.17 ± 0.16^{b}	7.00 ± 0.01^{c}	105 ± 4.1^{b}	85 ± 4.1^{b}
75 %-US	57.3 ± 0.9^{b}	57.4 ± 0.0^{c}	2.68 ± 0.14^{c}	6.90 ± 0.01^{c}	90 ± 8.2^{b}	85 ± 4.1^{b}
100 %-US	56.5 ± 0.9^{b}	55.6 ± 0.0^{c}	2.31 ± 0.10^{b}	6.73 ± 0.34^{c}	105 ± 4.1^{b}	85 ± 4.1^{b}

* Results are expressed as mean ± standard deviation. Different uppercase letters indicate statistically significant differences between mean values within the same column.

oil binding ability compared to the untreated sample (2.91 g/g). This is likely due to the controlled Maillard reaction, which modified and unfolded the protein structure, exposing more hydrophobic residues and thereby increasing the OBC of protein-dextran conjugates [22]. Once again, ultrasound treatment led to a significant enhancement, increasing OBC to 7.30 g/g compared to 5.74 g/g observed with dextran conjugation alone.

The foaming properties are largely dependent on the movement of proteins around air bubbles in the liquid phase and the rearrangement of molecules at the air-water interface [21]. Both foaming capacity (FC) and foaming stability (FS) notably increased when pea protein underwent dextran conjugation. Prior to conjugation, FC and FS were 52.5 % and 15 %, respectively, but rose up to 105 % and 85 % after conjugation. No significant differences were observed between ultrasound-treated and wet-heating alone.

3.7. Headspace volatiles and binding capacities of pea protein samples

The flavor compounds in the headspace of pea protein samples, analyzed using SIFT-MS, are presented in Table S1. Hexanal, an unpleasant grassy volatile compound with characteristic beany flavor was identified as the predominant aldehyde in the samples, followed by pentanal and octanal. Compared to the native (untreated) sample, the total aldehyde content decreased in the classical wet heating method (without ultrasound). However, the highest aldehyde concentration was observed at 25 % ultrasound amplitude. As the amplitude increased, aldehyde binding affinity improved, particularly at 100 % amplitude, leading to a reduction in headspace aldehyde content. Kong et al. [45] also reported a similar trend in soy protein, where aldehyde levels increased at low ultrasound power but decreased with increasing ultrasound intensity. This phenomenon was attributed to ultrasonic cavitation, which alters protein conformation, thereby disrupting the interactions between proteins and flavor compounds.

Analyzing the ketones, 2-octanone was initially the most dominant, accounting for 73 % of the total ketones. However, its concentration significantly decreased after dextran conjugation. This reduction was particularly pronounced in dextran conjugates produced with high ultrasound power, where 2-octanone levels dropped even below those of 2,3-butanedione at 100 % amplitude. 2-Octanone, known for its grassy and greenish notes, is directly associated with the characteristic "beany" flavor of pea protein [5,46]. Thus, it appears that this compound can be effectively trapped through conjugation and ultrasound treatment.

The controlled Maillard reaction, particularly during the Strecker degradation phase, may also contribute to flavor formation. Compounds such as furans, furan derivatives, pyrazines, and aldehydes can be generated through this process [45,47]. SIFT-MS headspace analysis showed that, in most cases, chemical modification resulted in lower levels of aldehydes and ketones, while promoting the release of alcohols, furan derivatives, pyrazines, and sulfur-containing compounds. The concentration of 5-hydroxymethylfurfural (HMF), a characteristic Maillard reaction product, increased notably with ultrasound treatment, reaching its peak at 25 % amplitude—a 72 % increase relative to the native protein.

Flavor formation in plant proteins can be both reversible and irreversible, depending on the type of modification and the stability of the formed compounds. On one hand, reactions contribute to the generation of new flavor compounds, while on the other, modified proteins also exhibit flavor-binding properties [40,48], making it challenging to isolate the specific effects of each process. To better understand the interaction between pea protein and volatile compounds, the binding capacity of the protein samples toward octanal and 2-octanone, representative aldehyde and ketone compounds, was evaluated under controlled conditions (Fig. 4A and B). These two volatiles share a similar carbon chain length (C8) and moderate hydrophobicity, both of which are critical factors influencing their interactions with proteins [49]. The octanol–water partition coefficient (log P) is commonly used to describe the hydrophobicity of flavor compounds and is often classified into low, moderate, and high hydrophobicity categories. The reported log *P* values of octanal and 2-octanone range from 2.54 to 2.78 and 2.37 to

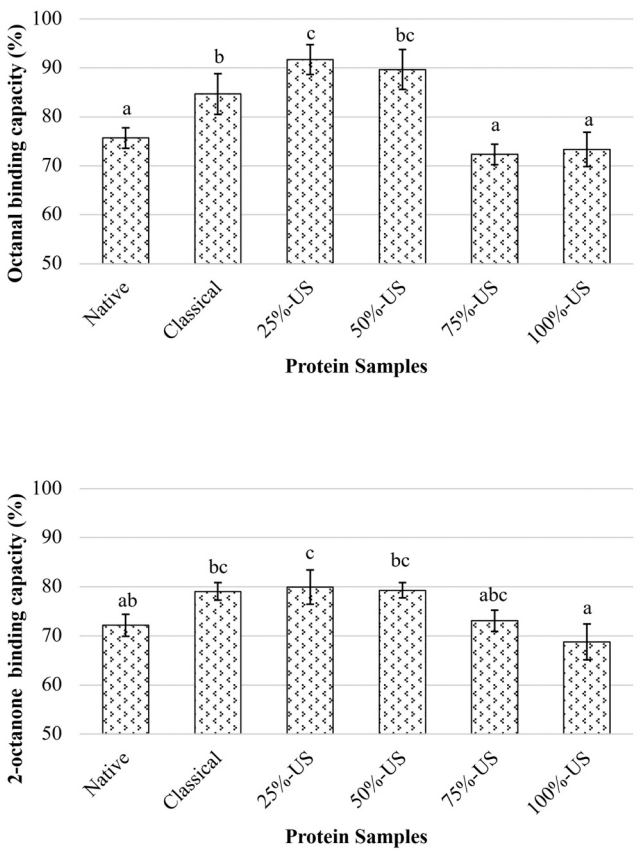

Fig. 4. Binding capacities of octanal (A) and 2-octanone (B) to pea protein samples, including native and dextran-conjugated forms (25 to 100 %-US: varied amplitudes of ultrasound). Different letters (a-c) indicate statistically significant differences ($P < 0.05$).

2.59, respectively [48,50], indicating that both compounds exhibit moderate hydrophobicity. According to the PubChem chemical database, their log P values are approximately 2.7 and 2.4, respectively.

In the aroma binding tests conducted in this study, where flavor compounds were freely added to the protein solutions, both compounds exhibited similar binding trends across different modification conditions. Dextran conjugation via wet heating enhanced the binding of both octanal and 2-octanone, with a peak observed at 25–50 % ultrasound amplitude, followed by a significant decline at 75 % and 100 % amplitudes ($P < 0.05$). The negative impact of high-intensity ultrasound on binding capacity was more pronounced for octanal, with the lowest binding levels observed at 75 % and 100 % amplitudes. Notably, octanal consistently showed higher binding affinity than 2-octanone, which may be partially attributed to its slightly higher log P value. In agreement with our findings, Li et al. [51] reported a higher proportion of unbound 2-octanone compared to octanal in modified myofibrillar protein systems. Similarly, two studies carried by Wang and Arntfield [50,52] observed greater octanal binding than 2-octanone. In our control samples, binding affinities were 72 % and 76 % for octanal and 2-octanone, respectively, whereas those studies reported 24 % and 62 % [52] and 19 % and 65–68 % [50] for the same volatiles bound to pea protein. These discrepancies can be explained by the complex nature of protein–flavor interactions, which are strongly influenced by factors such as the protein's structural characteristics, production process, pH, and other experimental parameters [51,53]. For instance, our volatile-to-protein ratio was 1 % (*w*/w), whereas the cited studies used 2.5 %. Additionally, our analysis employed SIFT-MS, while they used GC/MS, potentially contributing to methodological differences. Several studies underscore the multifaceted nature of protein–flavor interactions and highlight the absence of a universal mechanism [51]. Upon heating and mild sonication, partial unfolding of proteins may expose buried hydrophobic regions or interior binding sites, enhancing volatile retention. Conversely, possible protein aggregation induced by excessive ultrasound can lead to flavor release, thereby decreasing binding affinity [53].

Ultrasound-assisted Maillard conjugation may lead to structural modifications such as partial unfolding or exposure of internal hydrophobic regions [54], thereby increasing the accessibility and affinity of the protein for volatile compounds. Changes in secondary structure profiles (Fig. 2C) could support this hypothesis. Up to 25 % ultrasound amplitude, both α-helix and random coil contents increased, while β-sheet content decreased. This pattern may reflect partial unfolding and conformational rearrangement of the protein molecules, resulting in a more flexible structure with reduced ordered regions. Additionally, DSC results revealed a decrease in denaturation temperature (Tp) and enthalpy (ΔH), which may suggest a reduction in thermal stability, possibly due to conformational alterations or loosening of the protein matrix [53]. Zeta potential changes also reflect surface charge redistribution, potentially due to exposure of charged or polar residues upon unfolding. These changes were significantly correlated with flavor-binding capacities of both octanal and 2-octanone, as shown by Pearson's correlation analysis (Fig. S1). Distinct from octanal, 2-octanone binding additionally correlated with WHC, a property linked to protein aggregation and network formation, potentially affecting aroma retention [48]. Our results demonstrate that protein–flavor interactions can be optimized via controlled conjugation, with 25 % US amplitude emerging as the most effective condition. These findings emphasize not only the benefits of conjugation but also the critical importance of optimizing ultrasound intensity.

4. Conclusions

Ultrasound demonstrated its ability to facilitate dextran conjugation and enhance techno-functional properties. Medium-power ultrasound (25 %) induced structural unfolding and conformational changes in pea protein, resulting in a decrease in the relative proportions of *β*-sheet and an increase in the α-helix and random coil. Unlike previous studies, this research observed a decrease in the absolute zeta potential, yet it exhibited a strong correlation with other parameters, providing robust evidence of conjugation and functional improvements. Chemical modification generally decreased the release of aldehydes and ketones while promoting the formation or release of alcohols, furan derivatives, pyrazines, and sulfur compounds, as detected by SIFT-MS headspace analysis. The flavor-binding capacities were strongly correlated with the degree of glycation, solubility, denaturation enthalpy, and protein conformation. Given that the flavor-binding property of proteins can sometimes be perceived negatively, future studies should explore the use of different flavorings to simulate model food systems.

CRediT authorship contribution statement

Fatih Mehmet Yılmaz: Writing – original draft, Validation, Methodology, Investigation, Formal analysis, Conceptualization. **Ahmet Görgüç:** Writing – original draft, Validation, Investigation, Formal analysis. **Sílvia de Lamo-Castellví:** Writing – review & editing, Methodology, Investigation. **Sheryl Barringer:** Writing – review & editing, Supervision, Methodology, Conceptualization.

Declaration of competing interest

The authors declare that they have no known competing financial interests or personal relationships that could have appeared to influence the work reported in this paper.

Acknowledgement

This research was supported by the Scientific and Technological Research Council of Türkiye (TÜBİTAK)-BİDEB through the '2219 International Postdoctoral Research Scholarship Program'. The authors also extend their gratitude to Dr. Rafael Jimenez-Flores, Dr. Emmanuel Hatzakis, Dr. Luis Rodriguez-Saona, and Mr. Matt Chrusciel for their support in providing access to specialized equipment.

Appendix A. Supplementary data

Supplementary data to this article can be found online at https://doi.org/10.1016/j.ijbiomac.2025.146607.

Data availability

Data will be made available on request.

References

[1] A. Choręziak, D. Rosiejka, J. Michałowska, P. Bogdański, Nutritional quality, safety and environmental benefits of alternative protein sources—an overview, Nutrients 17 (2025) 1148, https://doi.org/10.3390/nu17071148.
[2] J. Jing Fu, J. Xiu Yu, F. Yu He, Y. Na Huang, Z. Ping Wu, Y. Wen Chen, Physicochemical and functional characteristics of glycated collagen protein from giant salamander skin induced by ultrasound Maillard reaction, Int. J. Biol. Macromol. 254 (2024), https://doi.org/10.1016/j.ijbiomac.2023.127558.
[3] N. Babault, C. Païzis, G. Deley, L. Guérin-Deremaux, M.-H. Saniez, C. Lefranc-Millot, F.A. Allaert, Pea proteins oral supplementation promotes muscle thickness gains during resistance training: a double-blind, randomized, placebo-controlled clinical trial vs. whey protein, J. Int. Soc. Sports Nutr. 12 (2015), https://doi.org/10.1186/s12970-014-0064-5.
[4] Market Analysis Report, Plant based protein supplements market size, share & trends analysis report by raw material (soy, spirulina, pumpkin seed, wheat, hemp, rice, pea, others), by product, by distribution channel, by application, by region, and segment forecasts. Https://Www.Grandviewresearch.Com/Industry-Analysis/Plant-Based-Protein-Supplements-Market, 2023.
[5] F. Zha, K. Gao, J. Rao, B. Chen, Maillard-driven chemistry to tune the functionality of pea protein: structure characterization, site-specificity, and aromatic profile, Trends Food Sci. Technol. 114 (2021) 658–671, https://doi.org/10.1016/j.tifs.2021.06.029.
[6] A. Ochoa-Rivas, Y. Nava-Valdez, S.O. Serna-Saldívar, C. Chuck-Hernández, Microwave and ultrasound to enhance protein extraction from peanut flour under

alkaline conditions: effects in yield and functional properties of protein isolates, Food Bioproc. Tech. 10 (2017) 543–555, https://doi.org/10.1007/s11947-016-1838-3.
[7] F.C. de Oliveira, J.S. dos R. Coimbra, E.B. de Oliveira, A.D.G. Zuñiga, E.E.G. Rojas, Food protein-polysaccharide conjugates obtained via the Maillard reaction: a review, Crit. Rev. Food Sci. Nutr. 56 (2016) 1108–1125, https://doi.org/10.1080/10408398.2012.755669.
[8] K. Gao, Y. Xu, J. Rao, B. Chen, Maillard reaction between high-intensity ultrasound pre-treated pea protein isolate and glucose: impact of reaction time and pH on the conjugation process and the properties of conjugates, Food Chem. 434 (2024) 137486, https://doi.org/10.1016/j.foodchem.2023.137486.
[9] F. Zha, S. Dong, J. Rao, B. Chen, The structural modification of pea protein concentrate with gum Arabic by controlled Maillard reaction enhances its functional properties and flavor attributes, Food Hydrocoll. 92 (2019) 30–40, https://doi.org/10.1016/j.foodhyd.2019.01.046.
[10] X. Huang, C. Yan, M. Lin, C. He, Y. Xu, Y. Huang, Z. Zhou, The effects of conjugation of walnut protein isolate with polyphenols on protein solubility, antioxidant activity, and emulsifying properties, Food Res. Int. 161 (2022) 111910, https://doi.org/10.1016/j.foodres.2022.111910.
[11] I. Kutzli, D. Griener, M. Gibis, C. Schmid, C. Dawid, S.K. Baier, T. Hofmann, J. Weiss, Influence of Maillard reaction conditions on the formation and solubility of pea protein isolate-maltodextrin conjugates in electrospun fibers, Food Hydrocoll. 101 (2020) 105535, https://doi.org/10.1016/j.foodhyd.2019.105535.
[12] J. Jing Fu, F. Yu He, X. Tong Zhu, Z. Wang, Y. Na Huang, J. Xiu Yu, Z. Ping Wu, Y. Wen Chen, Structural characteristics and antioxidant activity of Chinese giant salamander enzymatic hydrolysate-glucose conjugates induced by ultrasound Maillard reaction, Food Biosci. 58 (2024), https://doi.org/10.1016/j.fbio.2024.103654.
[13] Z. Li, Y. Zheng, Q. Sun, J. Wang, B. Zheng, Z. Guo, Structural characteristics and emulsifying properties of myofibrillar protein-dextran conjugates induced by ultrasound Maillard reaction, Ultrason. Sonochem. 72 (2021), https://doi.org/10.1016/j.ultsonch.2020.105458.
[14] J. Zhang, C. Wen, Y. Duan, H. Zhang, H. Ma, Structure and functional properties of watermelon seed protein-glucose conjugates prepared by different methods, LWT 155 (2022), https://doi.org/10.1016/j.lwt.2021.113004.
[15] C. Hastie, A. Thompson, M. Perkins, V.S. Langford, M. Eddleston, N.Z.M. Homer, Selected ion flow tube-mass spectrometry (sift-ms) as an alternative to gas chromatography/mass spectrometry (gc/ms) for the analysis of cyclohexanone and cyclohexanol in plasma, ACS Omega 6 (2021) 32818–32822, https://doi.org/10.1021/acsomega.1c03827.
[16] D. Smith, P. Španěl, N. Demarais, V.S. Langford, M.J. McEwan, Recent developments and applications of selected ion flow tube mass spectrometry (SIFT-MS), Mass Spectrom. Rev. 44 (2025) 101–134, https://doi.org/10.1002/mas.21835.
[17] B. Başyiğit, M. Yücetepe, G. Akyar, A. Karaaslan, M. Karaaslan, Enhancing thermal and emulsifying resilience of pomegranate fruit protein with gum Arabic conjugation, Colloids Surf. B Biointerfaces 215 (2022), https://doi.org/10.1016/j.colsurfb.2022.112516.
[18] K. Rathnakumar, J. Ortega-Anaya, R. Jimenez-Flores, S.I. Martínez-Monteagudo, Improvements in the extraction of milk phospholipids from beta-serum using ultrasound prior to tertiary amine extraction, LWT 141 (2021) 110864, https://doi.org/10.1016/j.lwt.2021.110864.
[19] F. Zha, Z. Yang, J. Rao, B. Chen, Gum Arabic-mediated synthesis of glyco-pea protein hydrolysate via Maillard reaction improves solubility, flavor profile, and functionality of plant protein, J. Agric. Food Chem. 67 (2019) 10195–10206, https://doi.org/10.1021/acs.jafc.9b04099.
[20] A. Akyüz, İ. Tekin, Z. Aksoy, S. Ersus, Determination of process parameters and precipitation methods for potential large-scale production of sugar beet leaf protein concentrate, J. Sci. Food Agric. 104 (2024) 3235–3245, https://doi.org/10.1002/jsfa.13210.
[21] Ö. Erdoğdu, A. Görgüç, F.M. Yılmaz, Functionality enhancement of pea protein powder via high-intensity ultrasound: screening in-vitro digestion, o/w emulsion properties and testing in gluten-free bread, Plant Foods Hum. Nutr. 78 (2023) 597–603, https://doi.org/10.1007/s11130-023-01087-1.
[22] R. Rawat, C.S. Saini, Utilizing dry-heating Maillard reaction approach to modify the functional and structural properties of ultrasound pretreated Sunnhemp protein isolate with dextran, Food Bioproc. Tech. (2024), https://doi.org/10.1007/s11947-024-03547-1.
[23] A. Ballon, M.P. Romero, L.E. Rodriguez-Saona, S. de Lamo-Castellví, C. Güell, M. Ferrando, Conjugation of lesser mealworm (Alphitobius diaperinus) larvae protein with polyphenols for the development of innovative antioxidant emulsifiers, Food Chem. 434 (2024), https://doi.org/10.1016/j.foodchem.2023.137494.
[24] M. Kaur, S. Barringer, Effect of yogurt and its components on the deodorization of raw and fried garlic volatiles, Molecules 28 (2023) 5714, https://doi.org/10.3390/molecules28155714.
[25] Z. Hong, Y. Kong, R. Guo, Q. Huang, Stabilizing effect of silver carp myofibrillar protein modified by high intensity ultrasound on high internal phase emulsions: protein denaturation, interfacial adsorption and reconfiguration, Int. J. Biol. Macromol. 265 (2024) 130896, https://doi.org/10.1016/j.ijbiomac.2024.130896.
[26] Q. Zhang, L. Li, L. Chen, S. Liu, Q. Cui, W. Qin, Effects of sequential enzymolysis and glycosylation on the structural properties and antioxidant activity of soybean protein isolate, Antioxidants 12 (2023), https://doi.org/10.3390/antiox12020430.
[27] Y. Jiang, K. Zang, R. Yan, J. Sun, X. An Zeng, H. Li, C. Brennan, M. Huang, L. Xu, Modification of Jiuzao glutelin with pullulan through Maillard reaction: stability effect in nano-emulsion, in vitro antioxidant properties, and interaction with curcumin, Food Res. Int. 161 (2022), https://doi.org/10.1016/j.foodres.2022.111785.
[28] Z. Jiang, Y. Huangfu, L. Jiang, T. Wang, Y. Bao, W. Ma, Structure and functional properties of whey protein conjugated with carboxymethyl cellulose through maillard reaction, LWT 174 (2023), https://doi.org/10.1016/j.lwt.2022.114406.
[29] G. Karabulut, H. Feng, O. Yemiş, Physicochemical and antioxidant properties of industrial hemp seed protein isolate treated by high-intensity ultrasound, Plant Foods Hum. Nutr. 77 (2022) 577–583, https://doi.org/10.1007/s11130-022-01017-7.
[30] Q. Liu, H. Cui, B. Muhoza, K. Hayat, S. Hussain, M.U. Tahir, X. Zhang, C.T. Ho, Whey protein isolate-dextran conjugates: decisive role of glycation time dependent conjugation degree in size control and stability improvement of colloidal nanoparticles, LWT 148 (2021), https://doi.org/10.1016/j.lwt.2021.111766.
[31] K. Kotaska, J. Werle, B. Hosnedlova, R. Kizek, R. Prusa, Use of Fourier transform infrared (FTIR) spectroscopy to detect rarely occurring cyanoacrylate and pyrophosphate urine stones, Appl. Spectrosc. Rev. 58 (2023) 724–737, https://doi.org/10.1080/05704928.2022.2138423.
[32] S. Wei, H. Cui, K. Hayat, X. Zhang, C.-T. Ho, Glycine-xylose Amadori compound formation tracing through Maillard browning inhibition by 2-Threityl-thiazolidine-4-carboxylic acid formation from Deoxyosone and exogenous cysteine, J. Agric. Food Chem. 70 (2022) 12164–12171, https://doi.org/10.1021/acs.jafc.2c04961.
[33] P. Niederhafner, M. Šafařík, J. Neburková, T.A. Keiderling, P. Bouř, J. Šebestík, Monitoring peptide tyrosine nitration by spectroscopic methods, Amino Acids 53 (2021) 517–532, https://doi.org/10.1007/s00726-020-02911-7.
[34] H. Cui, Z. Zang, Q. Jiang, Y. Bao, Y. Wu, J. Li, Y. Chen, X. Liu, S. Yang, X. Si, B. Li, Utilization of ultrasound and glycation to improve functional properties and encapsulated efficiency of proteins in anthocyanins, Food Chem. 419 (2023) 135899, https://doi.org/10.1016/j.foodchem.2023.135899.
[35] Y. Chen, N. Zhang, X. Chen, Structurally modified polysaccharides: physicochemical properties, biological activities, structure–activity relationship, and applications, J. Agric. Food Chem. 72 (2024) 3259–3276, https://doi.org/10.1021/acs.jafc.3c06433.
[36] H. Chen, Z. Guo, Z. Wang, B. Yang, X. Chen, L. Wen, Q. Yang, J. Kan, Structural and physicochemical properties of the different ultrasound frequency modified Qingke protein, Ultrason. Sonochem. 94 (2023) 106338, https://doi.org/10.1016/j.ultsonch.2023.106338.
[37] J. Sun, Y. Mu, M. Obadi, S. Dong, B. Xu, Effects of single-mode microwave heating and dextran conjugation on the structure and functionality of ovalbumin–dextran conjugates, Food Res. Int. 137 (2020), https://doi.org/10.1016/j.foodres.2020.109468.
[38] S. Aravindakshan, T.H.A. Nguyen, C. Kyomugasho, A. Van Loey, M.E. Hendrickx, The rehydration attributes and quality characteristics of 'quick-cooking' dehydrated beans: implications of glass transition on storage stability, Food Res. Int. 157 (2022) 111377, https://doi.org/10.1016/j.foodres.2022.111377.
[39] J. Zhang, Q. Liu, Q. Chen, F. Sun, H. Liu, B. Kong, Synergistic modification of pea protein structure using high-intensity ultrasound and pH-shifting technology to improve solubility and emulsification, Ultrason. Sonochem. 88 (2022), https://doi.org/10.1016/j.ultsonch.2022.106099.
[40] Y. Xie, D. Chen, J. Cao, X. Wang, X. Yin, Synergistic effects of high-intensity ultrasound combined with L-lysine for the treatment of porcine myofibrillar protein regarding solubility and flavour adsorption capacity, Foods 13 (2024), https://doi.org/10.3390/foods13040629.
[41] H. Liu, H. Zhang, Q. Liu, Q. Chen, B. Kong, Solubilization and stable dispersion of myofibrillar proteins in water through the destruction and inhibition of the assembly of filaments using high-intensity ultrasound, Ultrason. Sonochem. 67 (2020) 105160, https://doi.org/10.1016/j.ultsonch.2020.105160.
[42] Y.H. Cheng, D.C. Mu, Y.Y. Feng, Z. Xu, L. Wen, M.L. Chen, J. Ye, Glycosylation of rice protein with dextran via the Maillard reaction in a macromolecular crowding condition to improve solubility, J. Cereal Sci. 103 (2022), https://doi.org/10.1016/j.jcs.2021.103374.
[43] J. Mao, Y. Gao, Z. Meng, Regulation of fat crystals in water-in-oil emulsions by high-intensity ultrasound: crystal size and tracing of droplet distribution, Food Res. Int. 188 (2024), https://doi.org/10.1016/j.foodres.2024.114493.
[44] Y. Xu, M. Han, M. Huang, X. Xu, Enhanced heat stability and antioxidant activity of myofibrillar protein-dextran conjugate by the covalent adduction of polyphenols, Food Chem. 352 (2021), https://doi.org/10.1016/j.foodchem.2021.129376.
[45] Y. Kong, L. Sun, Z. Wu, Y. Li, Z. Kang, F. Xie, D. Yu, Effects of ultrasonic treatment on the structural, functional properties and beany flavor of soy protein isolate: comparison with traditional thermal treatment, Ultrason. Sonochem. 101 (2023) 106675, https://doi.org/10.1016/j.ultsonch.2023.106675.
[46] S. Vatansever, B. Chen, C. Hall, Plant protein flavor chemistry fundamentals and techniques to mitigate undesirable flavors, Sustain. Food Proteins 2 (2024) 33–57, https://doi.org/10.1002/sfp2.1025.
[47] Y. Yu, C. Fan, J. Qi, X. Zhao, H. Yang, G. Ye, M. Zhang, D. Liu, Effect of ultrasound treatment on porcine myofibrillar protein binding furan flavor compounds at different salt concentrations, Food Chem. 443 (2024) 138427, https://doi.org/10.1016/j.foodchem.2024.138427.
[48] S. Saffarionpour, Off-flavors in pulses and grain legumes and processing approaches for controlling flavor-plant protein interaction: application prospects in plant-based alternative foods, Food Bioproc. Tech. 17 (2024) 1141–1182, https://doi.org/10.1007/s11947-023-03148-4.
[49] C. Barallat-Pérez, H.G. Janssen, S. Martins, V. Fogliano, T. Oliviero, Unraveling the role of flavor structure and physicochemical properties in the binding phenomenon with commercial food protein isolates, J. Agric. Food Chem. 71 (2023) 20274–20284, https://doi.org/10.1021/acs.jafc.3c05991.

[50] K. Wang, S.D. Arntfield, Probing the molecular forces involved in binding of selected volatile flavour compounds to salt-extracted pea proteins, Food Chem. 211 (2016) 235–242, https://doi.org/10.1016/j.foodchem.2016.05.062.
[51] H. Li, R. Zheng, F. Zuo, C. Qian, Z. Yao, R. Dong, D. Zhao, C. Li, Influence of proteolysis on the binding capacity of flavor compounds to Myofibrillar proteins, Foods 11 (2022), https://doi.org/10.3390/foods11060891.
[52] K. Wang, S.D. Arntfield, Modification of interactions between selected volatile flavour compounds and salt-extracted pea protein isolates using chemical and enzymatic approaches, Food Hydrocoll. 61 (2016) 567–577, https://doi.org/10.1016/j.foodhyd.2016.05.040.
[53] K. Wang, S.D. Arntfield, Effect of protein-flavour binding on flavour delivery and protein functional properties: a special emphasis on plant-based proteins, Flavour Fragr. J. 32 (2017) 92–101, https://doi.org/10.1002/ffj.3365.
[54] S. Aziznia, G. Askari, Z. Emamdjomeh, M. Salami, Effect of ultrasonic assisted grafting on the structural and functional properties of mung bean protein isolate conjugated with maltodextrin through maillard reaction, Int. J. Biol. Macromol. 254 (2024), https://doi.org/10.1016/j.ijbiomac.2023.127616.